Available online at www.sciencedirect.com
ScienceDirect
Ceramics International 34 (2008) 421–427
CERAMICS INTERNATIONAL
www.elsevier.com/locate/ceramint

Formation of $LiNi_{0.5}Co_{0.5}VO_4$ nano-crystals by solvothermal reaction

Titipun Thongtem *, Anukorn Phuruangrat, Somchai Thongtem

Faculty of Science, Chiang Mai University, Chiang Mai 50200, Thailand

Received 29 August 2006; received in revised form 28 September 2006; accepted 1 November 2006
Available online 14 December 2006

Abstract

$LiNi_{0.5}Co_{0.5}VO_4$ nano-crystals were solvothermally prepared using a mixture of $LiOH{\cdot}H_2O$, $Ni(NO_3)_2{\cdot}6H_2O$, $Co(NO_3)_2{\cdot}6H_2O$ and NH_4VO_3 in isopropanol at 150–200 °C followed by 300–600 °C calcination to form powders. TGA curves of the solvothermal products show weight losses due to evaporation and decomposition processes. The purified products seem to form at 500 °C and above. The products analyzed by XRD, selected area electron diffraction (SAED), energy dispersive X-ray (EDX) and atomic absorption spectrophotometer (AAS) correspond to $LiNi_{0.5}Co_{0.5}VO_4$. V–O stretching vibrations of VO_4 tetrahedrons analyzed using FTIR and Raman spectrometer are in the range of 620–900 cm^{-1}. A solvothermal reaction at 150 °C for 10 h followed by calcination at 600 °C for 6 h yields crystals with lattice parameter of 0.8252 ± 0.0008 nm. Transmission electron microscope (TEM) images clearly show that the solvothermal temperatures play a more important role in the size formation than the reaction times.

Keywords: $LiNi_{0.5}Co_{0.5}VO_4$; Nano-crystals; Solvothermal reaction

1. Introduction

The development of new cathode materials for lithium batteries is increasingly important due to the use of portable electronic devices such as mobile phones, notebook computers and cameras [1,2]. Lithium transition metal oxides have inverse spinel structure and are very attractive for the use as cathode materials because they are able to give a voltage of 4.8 V [2–5]. There are several methods used for the preparation of these oxides. However, solid state reaction can lead to products with undesired properties [5,6]. To overcome these difficulties, low temperature wet chemistry methods have been developed [5–7]. At present, there are no reports on the preparation of $LiNi_{0.5}Co_{0.5}VO_4$ nano-crystals by solvothermal reaction with or without calcination at a variety of temperatures. Therefore, the nano-crystal oxide was prepared by this method and characterized to identify phase, morphology and other properties.

2. Experimental procedure

$LiNi_{0.5}Co_{0.5}VO_4$ nano-crystals were solvothermally prepared using a mixture of $LiOH{\cdot}H_2O$, $Ni(NO_3)_2{\cdot}6H_2O$, $Co(NO_3)_2{\cdot}6H_2O$ and NH_4VO_3 in isopropanol at 150–200 °C for 10–360 h. The products were subsequently calcined at 300–600 °C for 6 h to form powders (Fig. 1). They were analyzed using a thermogravimetric analyzer (TGA) with a heating rate of 20 °C min^{-1} in 100 ml min^{-1} N_2, an X-ray diffractometer (XRD) operated at 20 kV, 15 mA, using the Kα line from a Cu target, a transmission electron microscope (TEM) as well as selected area electron diffraction (SAED) operated at 200 kV, a Fourier transform infrared spectrometer (FTIR) with KBr as a diluting agent and operated in the range 400–4000 cm^{-1}, a Raman spectrometer using 30 mW He–Ne laser with $\lambda = 632.8$ nm, an energy dispersive X-ray (EDX) analyzer operated at 15 kV, and an atomic absorption spectrophotometer (AAS) to determine Ni:Co atomic ratios.

3. Results and discussion

3.1. TGA

Solvothermal products were analyzed using TGA. The weight losses are shown in Fig. 2. There are two steps of weight losses due to the evaporation of water at 38–172 °C, and the decomposition and combustion of residual starting agents at 172–500 °C. Weight losses decreased with the increase of solvothermal temperatures and reaction times showing that

---

* Corresponding author.
E-mail addresses: ttpthongtem@yahoo.com, ttpthongtem@hotmail.com (T. Thongtem).

0272-8842/$34.00
doi:10.1016/j.ceramint.2006.11.001

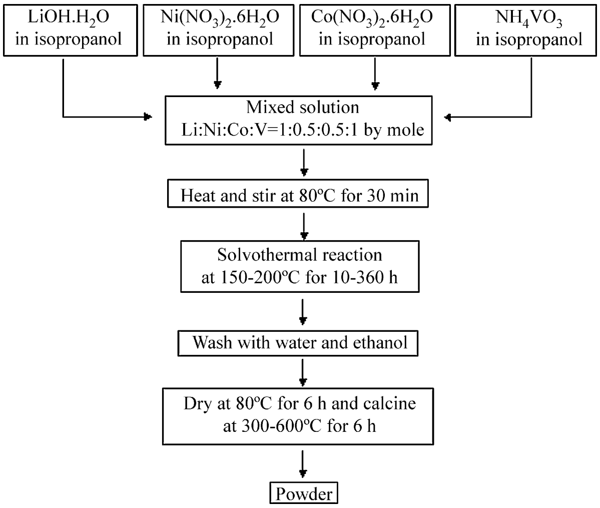

Fig. 1. Diagram used for preparation of $LiNi_{0.5}Co_{0.5}VO_4$.

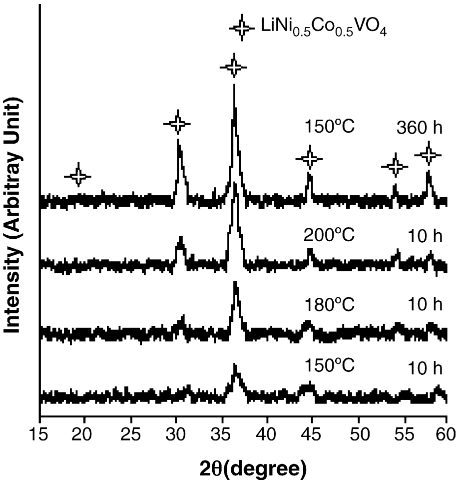

Fig. 3. XRD spectra of the solvothermal products prepared at a variety of temperatures and times.

higher temperatures and prolonged times promote the product formation. Weight percents are constant at 500–850 °C showing that purified products seem to form at these temperatures.

3.2. XRD

XRD spectra of the products prepared by solvothermal reaction with and without high temperature calcination are shown in Figs. 3 and 4. The spectra correspond to those of $LiNi_{0.5}Co_{0.5}VO_4$ [4,5] and are very close to those of the JCPDS standard for $LiNiVO_4$ and $LiCoVO_4$ [8]. Therefore, the products are verified to be $LiNi_{0.5}Co_{0.5}VO_4$. The strongest intensity peak diffracts from the (3 1 1) plane of the products. The (2 2 0) peak is higher than the (1 1 1) peak showing that the products have inverse spinel structure [2,4]. In addition, the degree of crystallinity is improved by the higher temperatures and prolonged times of the solvothermal reaction, as well as the calcination temperatures. Calculated lattice parameter of $LiNi_{0.5}Co_{0.5}VO_4$ prepared by 150 °C solvothermal reaction for 10 h followed by 600 °C calcination for 6 h is 0.8252 ± 0.0008 nm [9] which is very close to the values shown in the JCPDS standard (0.8220 nm for $LiNiVO_4$ and 0.8279 nm for $LiCoVO_4$) [8]. It is also in accord with those of $LiNi_{1-y}Co_yVO_4$ ($0 \leq y \leq 1$) which were prepared by a solid state reaction of Li_2CO_3, NiO, Co_3O_4 and V_2O_5 at 800 °C for 20 h [3]. Calculated lattice parameters of $LiNiVO_4$ and $LiCoVO_4$ are 0.8227 and 0.8287 nm [3], respectively. Those of $LiNiVO_4$–$LiCoVO_4$ solid solution are between the two values [3]. This shows that the reaction temperature and time have no influence on the lattice parameter of the product.

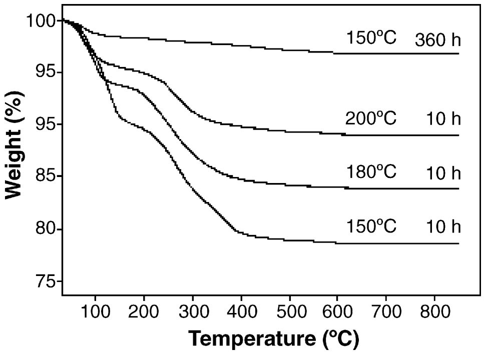

Fig. 2. TGA curves of solvothermal products prepared at a variety of temperatures and times.

3.3. TEM

TEM images of the products prepared under a variety of conditions are shown in Fig. 5. The sizes of the crystals were measured along 10 straight lines drawn in random directions.

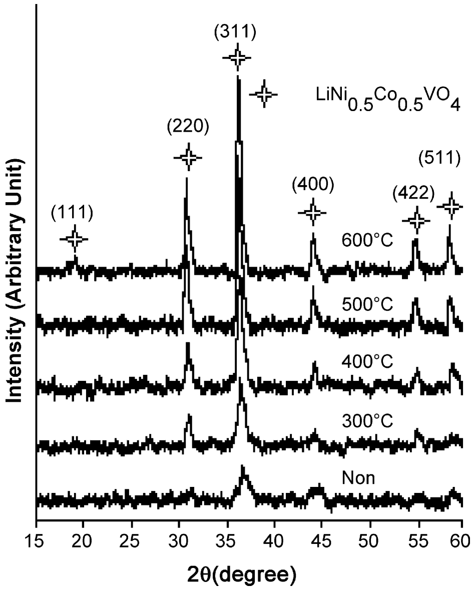

Fig. 4. XRD spectra of the products prepared by solvothermal reaction at 150 °C for 10 h with and without calcination at 300–600 °C for 6 h.

Average and standard deviation were calculated. The solvothermal reaction at 150 °C for 10 h yielded a product composed of very fine round crystals with size of 11.31 ± 2.38 nm. When the solvothermal time was prolonged to 360 h, the resulting crystals were almost at the same sizes (11.44 ± 1.87 nm) and shapes. At 180 and 200 °C for 10 h, the crystals are 16.19 ± 3.88 and 19.00 ± 3.97 nm in size, respectively. This shows that solvothermal temperatures play a more important role in the size than prolonged reaction times. The crystals were gradually improved by a 10 h solvothermal reaction at higher temperatures. The solvothermal reaction at 150 °C for 10 h and subsequent calcination at 300 and 600 °C

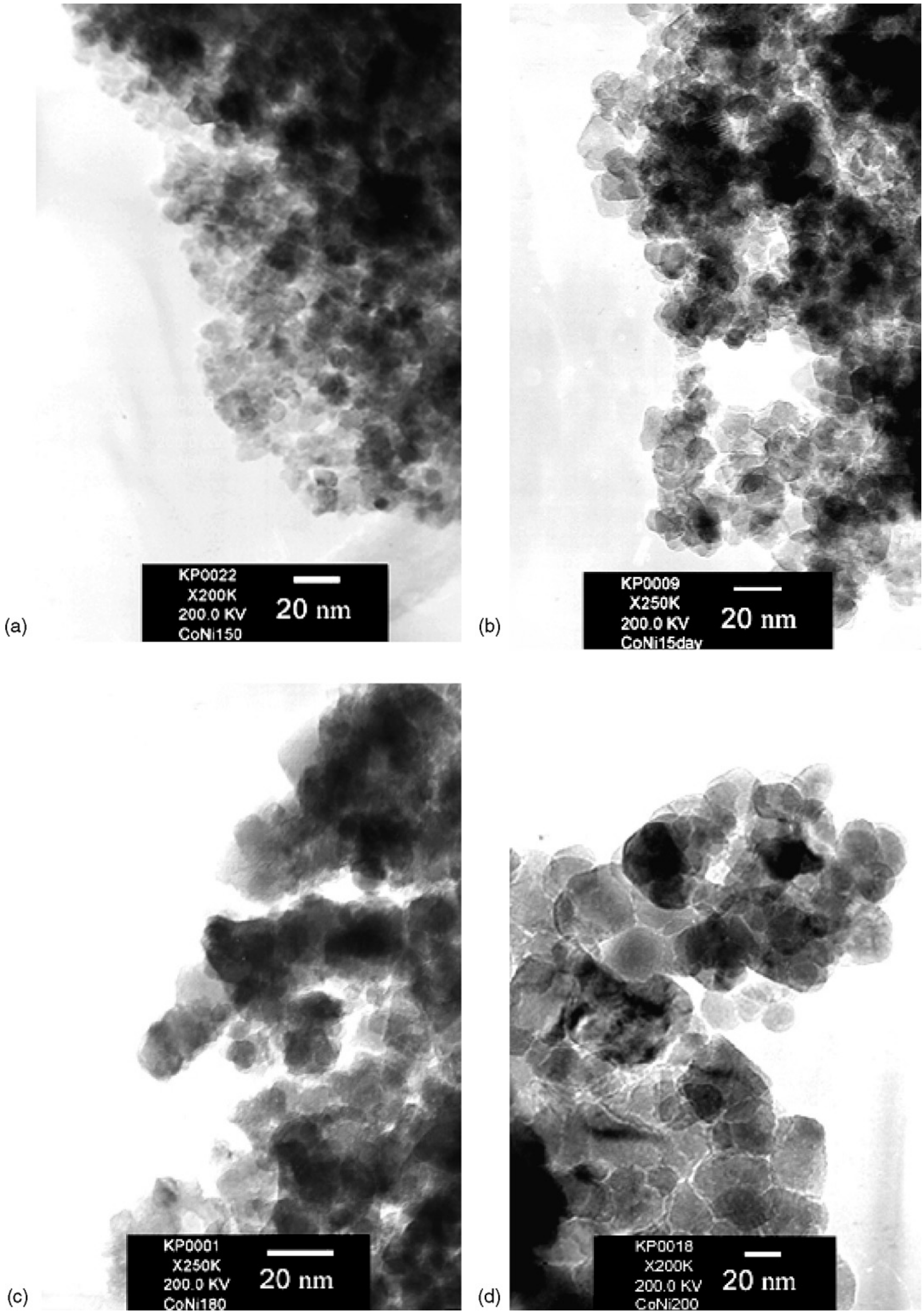

Fig. 5. TEM images of the products respectively prepared by: (a and b) 150 °C solvothermal reaction for 10 and 360 h; (c and d) 180 and 200 °C solvothermal reaction for 10 h; (e and f) 150 °C solvothermal reaction for 10 h followed by 300 and 600 °C calcination for 6 h.

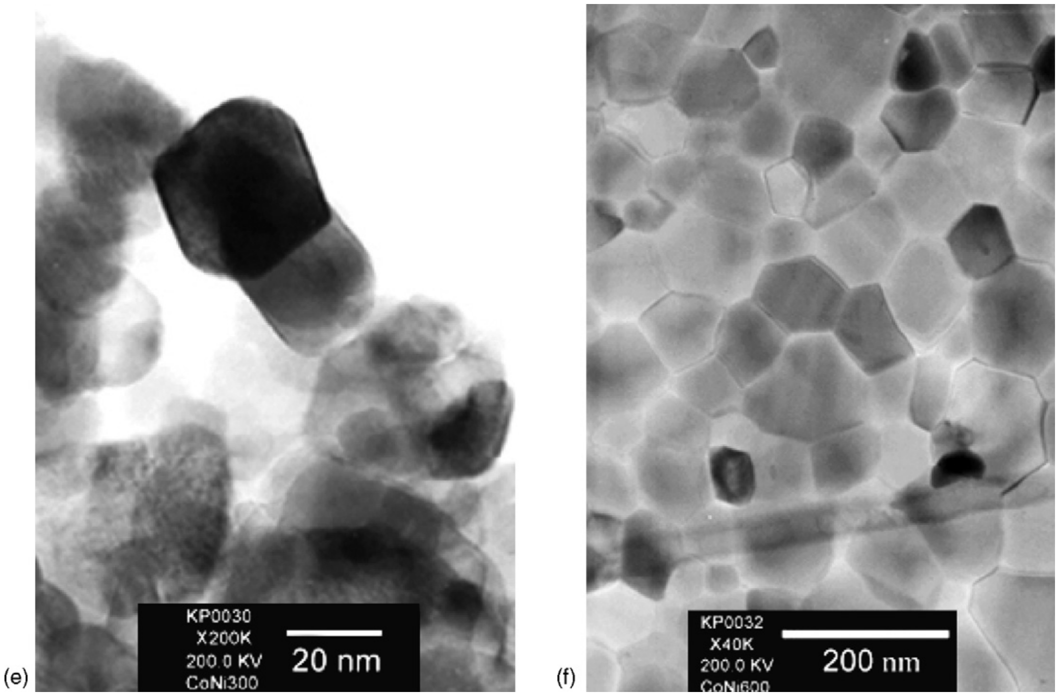

Fig. 5. (*Continued*).

for 6 h, led to crystals which are much bigger in size and the facets are clearer than the former. Sizes are 27.70 ± 9.63 and 98.44 ± 29.10 nm, respectively. $LiNi_yCo_{1-y}VO_4$ ($0 \leq y \leq 1$) crystals which were prepared by solid state reaction of Li_2CO_3, NiO, Co_3O_4 and V_2O_5 at high temperature, showed non-uniform sizes [10,11]. The particles were in the range of 5–30 μm depending on the Co content. They were much larger than those prepared by the described solvothermal reaction.

3.4. SAED

SAED patterns of the products are shown in Fig. 6. A number of bright spots are arranged into seven concentric rings corresponding to the diffraction planes of the products. The crystals become larger at higher reaction temperatures and therefore their coverage by the aperture is lesser in number. This leads to a greater degree of ring discontinuity. The interplanar spaces between the diffraction planes were calculated [12] and found to be very close to those of the JCPDS standard for both $LiNiVO_4$ and $LiCoVO_4$ [8]. The products were identified as $LiNi_{0.5}Co_{0.5}VO_4$ [5] and the diffraction planes are (1 1 1), (2 2 0), (3 1 1), (4 0 0), (4 2 2), (5 1 1) and (4 4 0). The findings show that SAED and XRD analyses are in perfect accord.

3.5. FTIR

FTIR spectra of the products prepared by solvothermal reaction with and without calcination at high temperatures are shown in Figs. 7 and 8. For the solvothermal reaction alone, the product spectra show a broad band of O–H stretching of residual water at 3070–3680 cm^{-1}, and O–H bending of water at 1590–1690 cm^{-1}. N–O stretching and N–H bending bands of residual nitrate and ammonium ions of the starting agents were detected at 1340–1400 cm^{-1} [13,14]. The vibrations of these bands were also detected by the individual FTIR analysis of $Ni(NO_3)_2{\cdot}6H_2O$, $Co(NO_3)_2{\cdot}6H_2O$ and NH_4VO_3 (results not shown). The broad band of V–O stretching of VO_4 tetrahedrons was detected at 620–900 cm^{-1} [1,2,7]. When the solvothermal temperatures and times were increased, these bands were still present. The solvothermal reaction at 150 °C for 10 h with 300–600 °C calcination for 6 h, yielded a product with decreased intensities of the spectra for O–H stretching and bending, N–O stretching, and N–H bending. These signals decrease with the increase of the calcination temperatures and no longer exist for products with 500 and 600 °C calcination temperatures.

3.6. Raman analysis

Raman spectra are shown in Fig. 9. Two strong peaks of V–O stretching of VO_4 tetrahedrons were detected at 814.5 and 788.1 cm^{-1} [3,4]. The first stretching frequency corresponds to A_{1g} symmetry [3,4]. The V–O bending of VO_4 tetrahedrons was detected at 324.8 cm^{-1} and has E_g symmetry [3,4]. Two stretching frequencies were detected at 472.9 and 405.1 cm^{-1} corresponding to the Li–O–M (M = Ni and Co) and Li–O stretching frequencies, respectively [3,4].

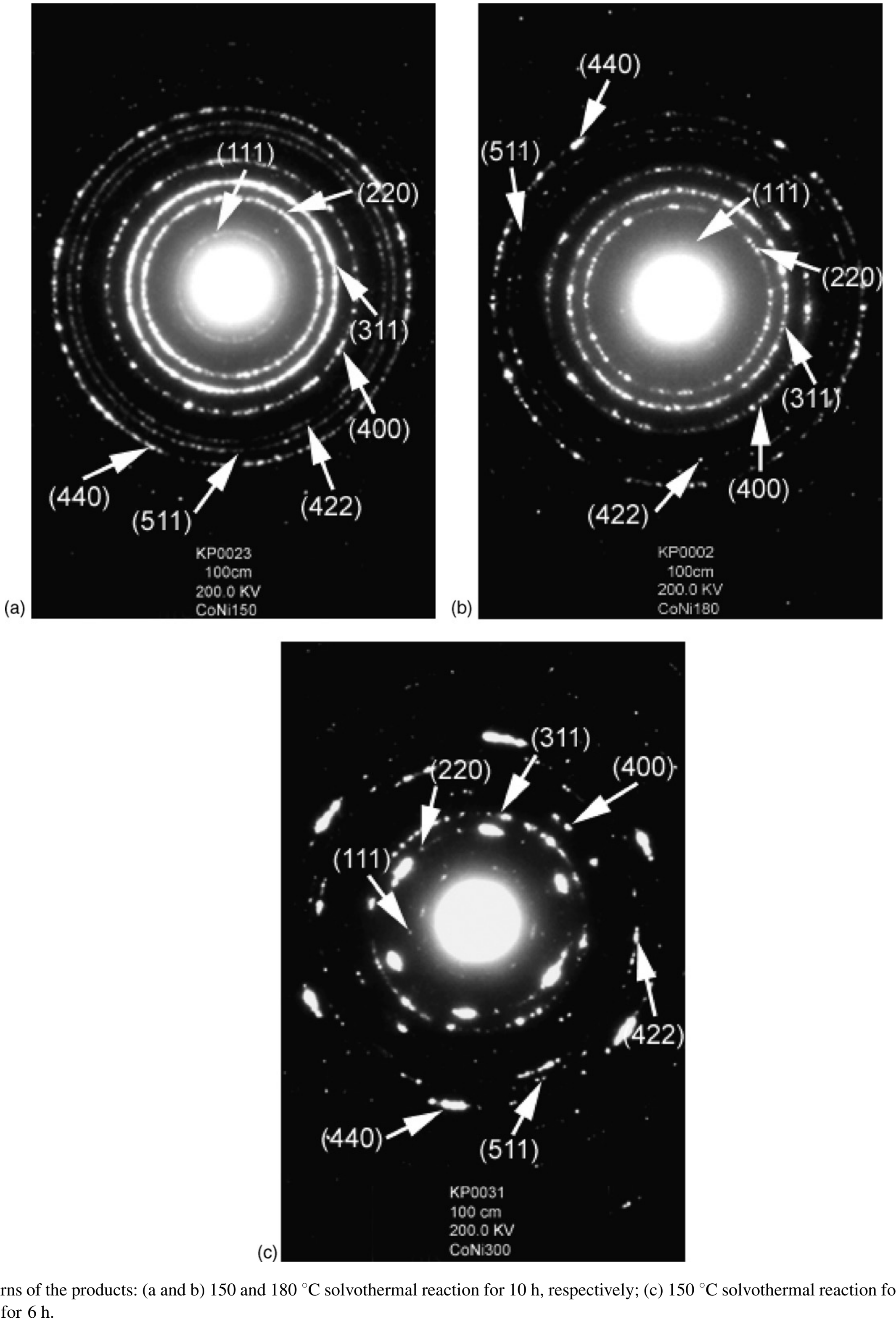

Fig. 6. SAED patterns of the products: (a and b) 150 and 180 °C solvothermal reaction for 10 h, respectively; (c) 150 °C solvothermal reaction for 10 h followed by 300 °C calcination for 6 h.

3.7. EDX and AAS

EDX analysis shown in Fig. 10 revealed the presence of Ni, Co, V and O. Li as the lightest metallic element was not detected. It indicates that EDX, XRD and SAED analyses are in accord. In addition, the products prepared by solvothermal reaction at 150 °C for 10 h followed by 500 and 600 °C calcination for 6 h were analyzed using AAS showing that Ni:Co atomic ratios are very close to 1:1.

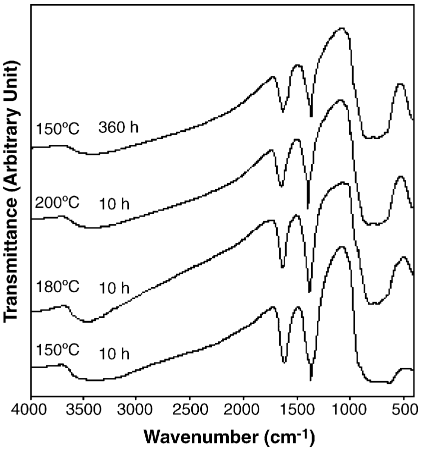

Fig. 7. FTIR spectra of the products prepared by solvothermal reaction at a variety of temperatures and times.

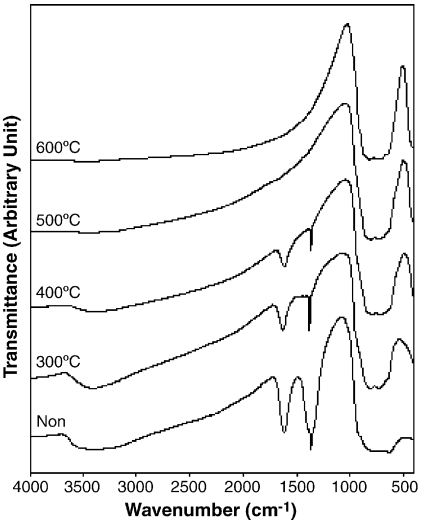

Fig. 8. FTIR spectra of the products prepared by solvothermal reaction at 150 °C for 10 h with and without calcination at 300–600 °C for 6 h.

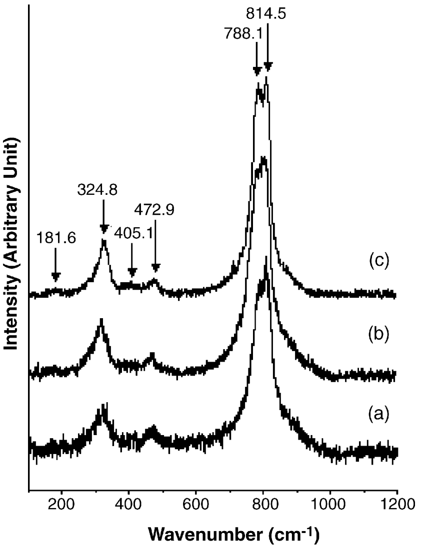

Fig. 9. Raman spectra: (a) 150 °C solvothermal reaction for 360 h; (b and c) 150 °C solvothermal reaction for 10 h followed by 300 and 600 °C calcination for 6 h, respectively.

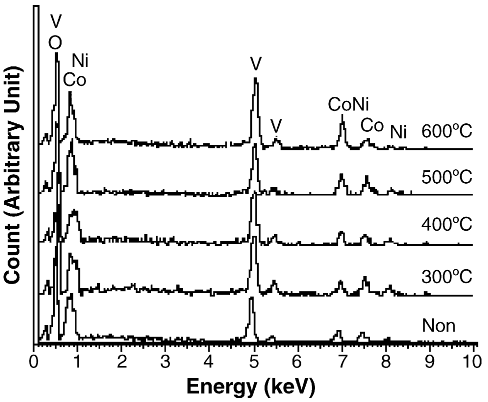

Fig. 10. EDX spectra of the products prepared by solvothermal reaction at 150 °C for 10 h with and without calcination at 300–600 °C for 6 h.

4. Conclusions

XRD, SAED, EDX and AAS revealed the formation of $LiNi_{0.5}Co_{0.5}VO_4$ prepared by 150–200 °C solvothermal reaction of a mixture of $LiOH{\cdot}H_2O$, $Ni(NO_3)_2{\cdot}6H_2O$, $Co(NO_3)_2{\cdot}6H_2O$ and NH_4VO_3 in isopropanol with and without calcination at 300–600 °C. V–O stretching peaks of the oxide were detected by FTIR at 620–900 cm^{-1} and Raman analysis at 814.5 and 788.1 cm^{-1}. TEM shows that the oxide is formed as nano-crystals which sizes are much increased with the increase of the calcination temperatures. TGA shows weight losses of two steps at 38–172 and 172–500 °C. Weight percents are constant at 500 °C and above.

Acknowledgements

The research was supported by the National Research Council of Thailand, and National Nanotechnology Center, Thailand.

References

[1] C.H. Lu, W.C. Lee, S.J. Liou, G.T.K. Fey, Hydrothermal synthesis of $LiNiVO_4$ cathode material for lithium ion batteries, J. Power Sources 81–82 (1999) 696–699.

[2] W. Chen, L.Q. Mai, Q. Xu, Q.Y. Zhu, H.P. Yang, Novel soft solution synthesis and characterization of submicromic $LiCoVO_4$, Mater. Sci. Eng. B 100 (2003) 221–224.

[3] C. Julien, M. Massot, C. Pérez-Vicente, Structural and vibrational studies of $LiNi_{1-y}Co_yVO_4$ $(0 \leq y \leq 1)$ cathodes materials for Li-ion batteries, Mater. Sci. Eng. B 75 (2000) 6–12.

[4] G.T.K. Fey, D.L. Huang, Synthesis, characterization and cell performance of inverse spinel electrode materials for lithium secondary batteries, Electrochim. Acta 45 (1999) 295–314.

[5] S. Vivekanandhan, M. Venkateswarlu, N. Satyanarayana, Effect of different ethylene glycol precursors on the Pechini process for the synthesis of nano-crystalline $LiNi_{0.5}$ $Co_{0.5}VO_4$ powders, Mater. Chem. Phys. 91 (2005) 54–59.

[6] S. Vivekanandhan, M. Venkateswarlu, N. Satyanarayana, Glycerol-assisted gel combustion synthesis of nano-crystalline $LiNiVO_4$ powders for secondary lithium batteries, Mater. Lett. 58 (2004) 1218–1222.

[7] C.H. Lu, S.J. Liou, Hydrothermal preparation of nanometer lithium nickel vanadium oxide powder at low temperature, Mater. Sci. Eng. B 75 (2000) 38–42.

[8] Powder Diffraction File, JCPDS International Centre for Diffraction Data, PA 19073-3273, U.S.A., 2001.

[9] C. Suryanarayana, M.G. Norton, X-Ray Diffraction, A Practical Approach, Plenum Press, New York, 1998, pp. 97–101.

[10] G.T.K. Fey, K.S. Wang, S.M. Yang, New inverse spinel cathode materials for rechargeable lithium batteries, J. Power Sources 68 (1997) 159–165.

[11] M.S. Bhuvaneswari, S. Selvasekarapandian, O. Kamishima, J. Kawamura, T. Hattori, Synthesis and structural analysis of lithium nickel vanadate, Mater. Chem. Phys. 91 (2005) 94–98.

[12] K.W. Andrews, D.J. Dyson, S.R. Keown, Interpretation of Electron Diffraction Patterns, Plenum Press, New York, 1971, pp. 14–15.

[13] B. Smith, Infrared Spectral Interpretation, A Systematic Approach, CRC Press, New York, 1999.

[14] K. Nakamoto, Infrared and Raman Spectra of Inorganic and Coordination Compounds, Part B, fifth ed., John Wiley & Sons, New York, 1997.